Experimental Determination of Processing-Induced Stresses and Properties of Graded Nickel-Alumina Coatings

by

Olivera E. Kesler

Submitted to the Department of Materials Science and Engineering
in partial fulfillment of the requirements for the degree of

Master of Science in Materials Science and Engineering

at the

MASSACHUSETTS INSTITUTE OF TECHNOLOGY

June 1997

Author .....
Department of Materials Science and Engineering
May 9, 1997

Certified by .....
Subra Suresh
R. P. Simmons Professor of Materials Science and Engineering
Thesis Supervisor

Accepted by .....
Linn W. Hobbs
Chairperson, Department Committee on Graduate Students

Experimental Determination of Processing-Induced Stresses and Properties of Graded Nickel-Alumina Coatings

by

Olivera E. Kesler

Submitted to the Department of Materials Science and Engineering
on May 9, 1997, in partial fulfillment of the
requirements for the degree of
Master of Science in Materials Science and Engineering

Abstract

An experimental determination of processing-induced intrinsic stresses and coefficients of thermal expansion has been made on plasma-sprayed Ni-alumina surface coatings of homogeneous and graded compositions. The results are obtained using a new experimental technique developed as part of the author's doctoral research work in which a number of identical substrate specimens are coated simultaneously with surface layers of fixed or graded compositions, and specimens with different layer thicknesses are periodically removed from the deposition chamber. Laser-scanning curvature measurements are performed on each of the specimens at room temperature and at elevated temperatures. From these experimental measurements, the residual processing-induced stress at room temperature and the coefficient of thermal expansion are calculated for each specimen. The knowledge of the coefficient of thermal expansion and room temperature residual stress are used to separate and calculate the individual effects of the thermal mismatch stress, induced upon cooling to room temperature, and the intrinsic quenching stress created at the processing temperature. The Young's modulus of each of the deposited materials used in the residual stress determinations was obtained by a rule of mixtures calculation, in which the values of the Young's modulus taken for each of the end components reflect the decrease in modulus observed in the literature in materials with a high level of porosity produced by the plasma spraying process. The intrinsic quenching stresses are found to be everywhere tensile, and significantly higher in materials deposited on similar sublayers (metal on metal or ceramic on ceramic) than in ceramic materials deposited directly on metal. The thermal mismatch stress produced during cooling to room temperature reduces the value of the tensile quenching stresses, however, reducing their absolute value and in some cases making the residual room temperature stresses slightly compressive.

Thesis Supervisor: Subra Suresh
Title: R. P. Simmons Professor of Materials Science and Engineering

Contents

List of Figures 5

List of Tables 6

Acknowledgements 7

1 Introduction 8

1.1 Functionally Graded Materials in Coatings 8

1.2 Overview 9

2 Background and Scope 11

2.1 Literature Review 11

2.2 Scope and Limitations of the Work 13

3 Experimental Procedure and Materials 16

3.1 Substrate preparation 16

3.2 Plasma-spray deposition 16

3.3 Curvature measurements 19

3.4 Four–point bend tests 19

4 Results and Discussion 23

4.1 Determination of Residual Stresses Using the Thin-Film Approximation 25

4.2 Determination of thermal expansion coefficient 26

4.3 Determination of residual stresses using the properties of the coatings 31

5 Conclusions and Future Work 34

Bibliography 36

List of Figures

3-1 Microstructure of Ni–Al_2O_3 graded coating. Steel substrate is at the bottom, and pure Al_2O_3 coating is at the top. 20

3-2 Microstructure of Ni–Al_2O_3 graded coating, showing the wavy nature of the layered deposits formed by plasma spraying. Ni is the light area, while Al_2O_3 is the darker area. 21

3-3 Microstructure of Ni–Al_2O_3 graded coatings showing details of the solidified Ni (lighter regions) and Al_2O_3 (darker regions) particles formed by plasma spray. 22

4-1 Total processing-induced residual stresses at room temperature in single graded layers of Ni–Al_2O_3, using thin film analysis. 27

4-2 Coefficient of thermal expansion of Ni–Al_2O_3 layers as a function of layer composition. 29

4-3 Coefficient of thermal expansion behavior of continuous fiber-reinforced composites [48]. 30

4-4 The separation of thermal mismatch, quenching, and total processing stresses in graded monolayers of Ni–Al_2O_3, using the rule of mixtures to estimate E. 32

List of Tables

3.1 Composition and thickness of specimens with coatings deposited in 20% incremented layers 18

4.1 Properties of the constituent phases of the graded coatings and substrate. 24

Acknowledgements

This work was supported by the Idaho National Engineering Laboratory Grant Agreement No. C95-175002-LKK-267-95, which is jointly funded at MIT and State University of New York (SUNY) at Stony Brook. This Grant is administered for the US Department of Energy by the Lockheed-Martin Corporation. Financial support for the author was provided by the National Defense Science and Engineering Graduate Fellowship Program, administered for the United States Department of Defense by the American Society for Engineering Education. The thermomechanical experiments and analyses reported here were carried out at the Laboratory for Experimental and Computational Micromechanics (LEXCOM) at MIT. Specimen preparation by plasma spray was carried out at the Thermal Spray Laboratory at SUNY, Stony Brook.

I would like to thank my thesis advisor, Professor Subra Suresh, for his guidance and constant support and encouragement during my studies. I also wish to thank my colleagues in LEXCOM for their support, and in particular, I wish to thank Dr. Marc Finot for his encouragement and many helpful discussions. I would also like to thank all of my friends who have made my time in graduate school so much more enjoyable. Finally, I wish to thank my family for their love and support through the years.

Chapter 1

Introduction

1.1 Functionally Graded Materials in Coatings

Structural coatings, with layer thicknesses of tens of micrometers to several millimeters, and thin-film coatings with layer thicknesses of tens of nanometers to several micrometers, are commonly used in a broad range of engineering components and electronic devices. Examples include protective layers to guard against thermal, environmental, corrosive, tribological or mechanical degradation of metallic structures, anti-reflective coatings on lenses, conductive metallic coatings on Si substrates in electronic devices, and thin magnetic coatings on metallic or polymeric substrates in information storage devices [1]. Advances in such processing methods as chemical vapor deposition, physical vapor deposition, thermal spray, powder metallurgy, computer-aided three-dimensional printing, self-propagating high-temperature combustion synthesis, electron-beam deposition and molecular beam epitaxy have given rise to newer opportunities for the synthesis of thick- and thin-film layered coatings [2]. In addition to surface coatings with homogeneous compositions which produce "sharp" interfaces among dissimilar solids, there is a growing interest in functionally graded materials wherein gradual changes in composition among dissimilar solids are produced across interfaces. The geometries of the graded interlayers are chosen

to mitigate internal stresses, enhance interfacial bonding, suppress the severity of stress concentrations at edges where interfaces intersect free surfaces, or to control the density and kinetics of misfit/threading dislocations emanating from interfaces [3-8].

All processing methods used to deposit surface coatings on substrates invariably generate "intrinsic" or "quench" stresses. These internal stresses, which strongly depend on the specific deposition conditions and processing methods employed, arise from such factors as: the rapid quenching of a molten droplet onto a substrate, non-uniform sintering of the material across the thickness of the coating, non-equilibrium cooling of the different phases, and epitaxial misfit strains. In addition, temperature excursions cause thermal stresses to develop due to expansion or contraction mismatch between the constituent phases in the same layer or between layers. A knowledge of these intrinsic processing stresses is crucial in designing coating materials that can withstand a prescribed in-service loading stress without failure. In addition, a knowledge of the connection between the processing conditions and the resulting values of residual stresses can be used to alter the processing conditions in order to minimize or optimize the initial stress state in the materials before they enter service. For example, spallation of a coating prior to a part entering service can be minimized by adjusting the processing conditions to optimize the residual stress state in the coating.

1.2 Overview

Chapter 2 provides a review of previous methods that have been used to determine residual stresses in thin film or homogeneous coatings, and the advantages of this method in the consideration of thick deposits and graded coatings. The experimental work is described in Chapter 3, and the results are presented and analyzed in Chapter 4. Chapter 5 presents a summary of the conclusions from this work and presents

additional research topics to be considered in future work.

Chapter 2

Background and Scope

2.1 Literature Review

A number of different approaches have been undertaken in the past to assess the intrinsic stresses produced by various deposition methods [9,10]. These include:

- Destructive methods which involve successive removal of the deposited layers and determination of the attendant changes in the strain or curvature of planar or cylindrical specimens [11-14].
- In-situ measurement of strain or curvature during thermal spray or epitaxial growth of thin films [15-22].
- X-ray or neutron diffraction to probe the changes in lattice constants, from which a measure of the internal stresses can be obtained [23-26].
- Optical fluorescence, in which piezo-spectroscopic effects are used to determine the internal stresses in optically transparent materials [27,28].

A major drawback of *a posteriori* stress assessment techniques, such as layer removal, is that grinding to remove deposits can induce surface compressive stresses, while etching can cause preferential and non-uniform chemical attack in a multi-

component, composite layer. Experimental difficulties in performing *in-situ* measurements may interfere with processing in many cases. Furthermore, the foregoing methods do not capture the redistribution of stresses through the thickness of the deposited layer during cooling from the processing temperature, and they do not isolate the quench stresses from the thermal stresses. While the depth of penetration into the coating by X-rays is small, both the X-ray and neutron diffraction methods suffer from the limitation that local plastic deformation as well as local variations in compositions, especially in the case of graded coatings, can elevate the uncertainty in stress estimates.

In view of these shortcomings of the available experimental methods, process modeling is often used to quantitatively derive the evolution of internal stresses for specific deposition techniques. Most such models are predicated upon first-principle calculations of the mechanics and physics of layer formation [29-32]. The key assumptions which enter into the analyses have not been directly checked with systematic experiments in most cases, and the complexity of various technologically significant processing methods causes the compounding of errors due to various approximations to such a degree that the reliability of the analysis becomes essentially intractable.

A lack of understanding of the processing-induced stresses renders the initial "mechanical condition" of the layered material to be unknown, even before it enters service [3-5]. As a result, subsequent thermomechanical reliability and life prediction analyses are prone to significant errors. This situation is further compounded by the fact that the thermal and mechanical properties of the surface coatings remain largely unexplored. In the few specific applications where detailed attempts have been made to determine the elastic moduli, thermal expansion coefficients and thermal conductivity of coatings, additional complications have been identified:

1. Layered coatings, produced by such commonly used methods as thermal spray, are markedly more compliant, less thermally conductive, more anisotropic, and

more porous when compared to bulk materials of the same composition [29,33-35].

2. The thermal and mechanical properties of the coatings can vary over the range of temperatures of practical interest.

3. While there exists some prior work (e.g., [36-38]) on the experimental measurement of the mechanical properties and residual stresses of homogeneous coatings, no "standard" methods of proven reliability are available to probe the properties of graded coatings.

4. To our knowledge, no experimental studies of the evolution of internal stresses during the processing of functionally graded coatings have been reported in the literature, and no procedures have thus far been formulated for the systematic evaluation of such properties as in-plane Young's modulus or coefficient of thermal expansion in graded coatings.

The objective of the present work was to determine the processing-induced stresses and thermal properties of layered and graded coatings in a model Ni-Al_2O_3 system, using new experimental and analytical tools developed as part of the author's doctoral thesis work [39-41]. Experimental confirmation of this method is provided with the aid of systematic measurements of intrinsic stresses and coefficient of thermal expansion for thermally-sprayed Ni–Al_2O_3 coatings of spatially homogeneous and graded compositions.

2.2 Scope and Limitations of the Work

The method used here enables the experimental determination of through-thickness variations in processing-induced stresses at room temperature, without altering the stress state during measurements, such as occurs in mechanically invasive techniques

such as layer removal and hole-drilling. The method also accounts for the thermal mismatch stresses induced by cooling from the processing temperature to room temperature, and isolates them from the intrinsic stresses produced by deposition.

The present method, however, has some limitations. The experiments are performed on deposited layers of finite thicknesses, and the calculations determine the average Young's modulus, coefficient of thermal expansion, and processing-induced stress for each layer or sublayer. Thus, the resolution of the through-thickness property determination of the coatings is limited by the smallest layer thickness which can still produce accurate measurements of E and α that can be distinguished from the measurements of the substrate properties alone. Experimentally, it is difficult to produce a continuously graded material, and a large number of measurements (typically involving ten or more sublayers) needs to be made in order to obtain the highest possible accuracy.

In addition, the process of interrupting the deposition to remove partially-coated specimens from the deposition chamber adds an intermediate cooling and heating step to the deposition procedure, which may, in some cases, alter the intrinsic stress distribution in layers (which are deposited on previous layers that have been cooled to room temperature and re-heated to the deposition temperature). However, because of the finite size of each deposited layer, it is likely that this effect would be pronounced only near the edges of each layer, and not near the middle of each deposit. And since the technique presented here measures the average stress in each layer, it is unlikely that this effect would significantly alter the determination of the average residual stresses in each deposited layer. Simple modifications to the specimen holder in the deposition chamber could also be designed which facilitate the removal of a single specimen (among a number of specimens) without any interruption in the deposition process.

The present method does not account for the variation in the Poisson ratio, ν,

through the thickness of the coated layer, which can introduce some errors in the estimates of the biaxial moduli. However, since ν variations span only a range of 0.26–0.32 for the materials considered in this work, this error is not expected to be significant.

In addition, α was assumed to be constant with temperature over the limited temperature range from processing to room temperature. This approximation is a reasonable one given the very nearly linear experimental relation between curvature and temperature of the specimens studied here.

The analyses employed here for the interpretation of stresses and material properties are predicated upon linear elasticity theory. Consequently, they provide accurate measures of stresses and properties only when the deposition conditions and subsequent thermal and mechanical loading do not induce plastic flow in the coating and the substrate.

Chapter 3

Experimental Procedure and Materials

3.1 Substrate preparation

Substrates for deposition were prepared from an SAE 1010 cold-rolled steel sheet (nominal composition 0.1 wt% C), by cutting the specimens into 19.1 mm x 50.8 mm x 0.7 mm plates, and polishing one side to obtain a reflective surface for the curvature measurements. The initial substrate curvatures were recorded using a Tencor FLX-2900 laser scanning device (Tencor Instruments, Mountain View, CA).

3.2 Plasma-spray deposition

Coatings were deposited on the steel substrate in an ambient atmosphere with an automated single-gun plasma-spray apparatus. Ni and Al_2O_3 powders were fed using two separate feeders, mixing the feed just prior to injection into the plasma spray torch, with the relative amounts of metal and ceramic adjusted in 5 percent increments to form a graded material beginning with Ni on the steel substrate and continuing in 5% increments to Al_2O_3 on the surface layer. For high concentrations of the ceramic

($\geq$ 60% Al_2O_3), the powders were pre-mixed prior to feeding to ensure sufficient mixing of the metal and ceramic. The substrates were preheated before each deposition to approximately 70°–100°C to obtain a relatively uniform temperature distribution during deposition. The substrate temperature during the deposition process was measured using an optical pyrometer, and was found to vary between 77°C and 158°C, with temperatures increasing gradually throughout the deposition process. During the deposition, the plasma torch was rastered across an area with dimensions slightly larger than that of a single specimen to increase the uniformity of the deposit thickness. Six specimens at a time were held magnetically on a rotating carousel and were rotated past the plasma gun.

The polished side of each substrate was protected with a cloth tape resistant to high temperatures to preserve the reflective surfaces for future curvature measurements. In addition, several of the substrates were exposed to various grit-blasting treatments to obtain a measurement of the resulting curvature change in the substrate due to the surface treatment alone. Grit-blasting is often used to roughen the surface of a substrate prior to deposition to allow better adhesion between the deposit and the substrate. The resulting change in curvature during grit-blasting was found to be much higher than the curvature resulting from the deposition, making the latter difficult to discern accurately if superimposed on the former. Therefore, the graded material layers were deposited directly onto the unpolished surface of the substrates, with no further surface treatment such as grit blasting applied prior to deposition. Despite the absence of a surface preparation prior to deposition, good adhesion was found between substrate and coating for every specimen except for that in which pure Al_2O_3 was deposited directly onto the steel.

The deposition process was stopped at 20% composition increments. Six substrates were inserted into the plasma spray chamber and a first layer of Ni–5 wt% Al alloy was deposited onto each steel substrate under identical processing conditions.

Specimen #	Ni/5 % Al	0-20 vol. % Al_2O_3	20-40 vol. % Al_2O_3	40-60 vol. % Al_2O_3	60-80 vol. % Al_2O_3	80-100 vol. % Al_2O_3	100 % Al_2O_3	steel substrate thickness (mm)	deposit thickness (mm)
1	•							0.645	0.069
2	•	•						0.673	0.282
3	•	•	•					0.665	0.529
4	•	•	•	•				0.671	0.708
5	•	•	•	•	•			0.671	1.112
6	•	•	•	•	•	•	•	0.663	1.554
7		•						0.668	0.226
8			•					0.671	0.266
9				•				0.671	0.221
10					•			0.668	0.422
11						•		0.673	0.246
12							•	0.665	0.181

Table 3.1: Composition and thickness of specimens with coatings deposited in 20% incremented layers

Then one specimen was removed from the chamber and replaced by a

new substrate. The remainder of the specimens were then deposited, all under identical conditions, with a second layer that was graded from 0% Al_2O_3 to 20% Al_2O_3. One of the original specimens was then removed, and the process was continued with each deposited layer containing a 20% increment in Al_2O_3 composition. Single-layer specimens, each with a graded layer within which the composition changes from one end of the layer to the other (specimens 7–12 in Table 3.1), as well as partially-formed graded coatings (specimens 1–6 in Table 3.1) were prepared.

Figure 3-1 shows the microstructure of a fully–graded deposit on steel ranging from Ni at the bottom to pure Al_2O_3 at the top. At higher magnifications (Figure 3-2 and

Figure 3-3), the microstructure of the deposited materials can be seen more clearly, with wavy individual splats of Ni and Al_2O_3 intermixed randomly, along with some porosity (in the range 6–12 volume per cent). As the composition of Al_2O_3 increases, the corresponding increase in the concentration of the Al_2O_3 splats is evident as the darker region in Figures 3-2 and 3-3.

3.3 Curvature measurements

The final curvature of each specimen was measured after deposition, and the initial curvature was subtracted to obtain the change in curvature due to the deposition process. In addition, each of the first batch of specimens was heated at 4°C/min to 100°C, held for one hour to allow an equilibrium steady state temperature to be reached, heated to 150°C, held for one hour again, and then cooled to room temperature to determine the change in curvature with temperature. The curvature measurements were performed on the Tencor FLX-2900 (Tencor Instruments, Mountain View, CA) laser scanning system. The curvature versus temperature data were used to determine the CTE and the intrinsic and residual stresses in the materials.

3.4 Four–point bend tests

Each of the specimens was then cut lengthwise using a Buehler Isomet 2000 precision saw, and two of these specimens, a bare steel substrate and the full FGM, were subjected to a four-point bending load in an Instron 4200 mechanical testing apparatus (Instron Corporation, Canton, MA), with the deflection of the specimens measured by crosshead displacement. The values of Young's modulus of the specimens were subsequently determined using the analysis in Section 4.3.

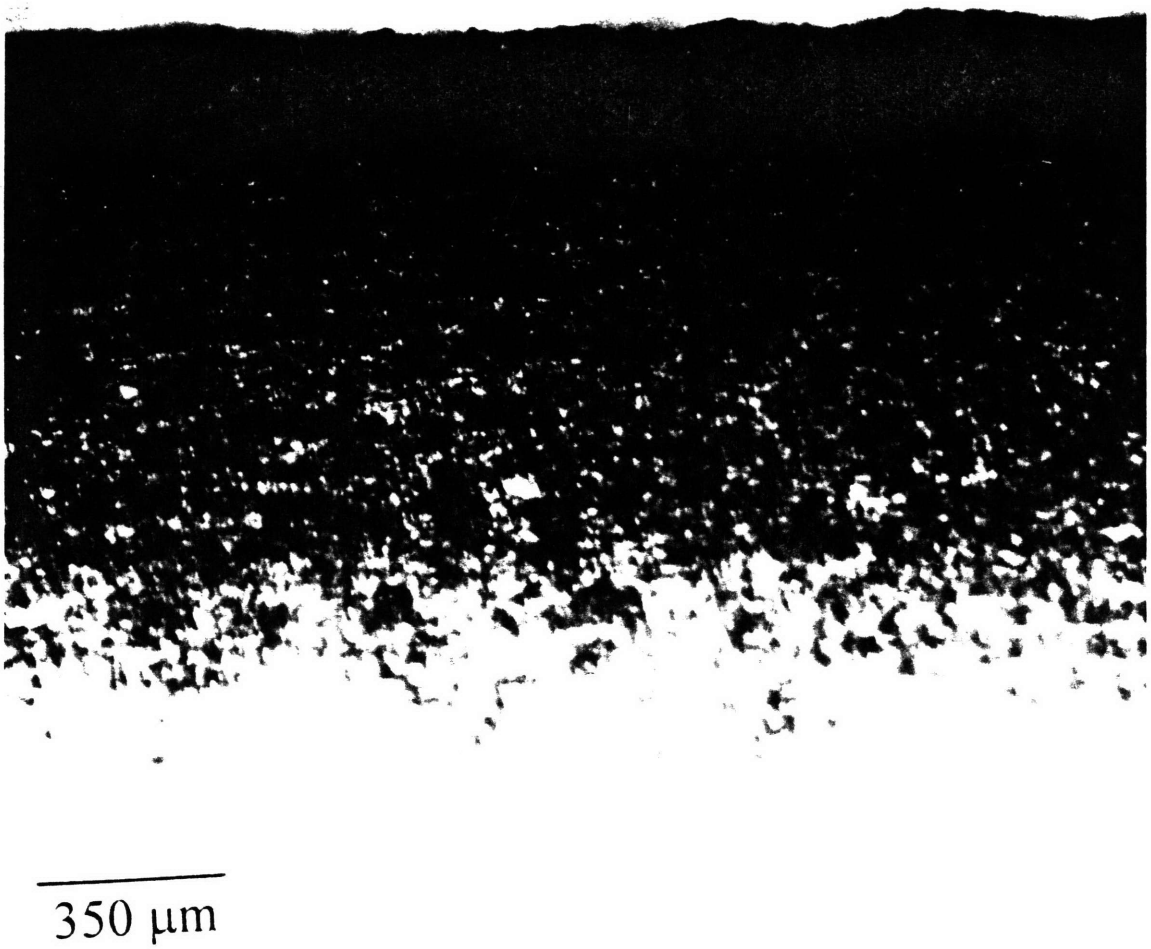

Figure 3-1: Microstructure of Ni–Al_2O_3 graded coating. Steel substrate is at the bottom, and pure Al_2O_3 coating is at the top.

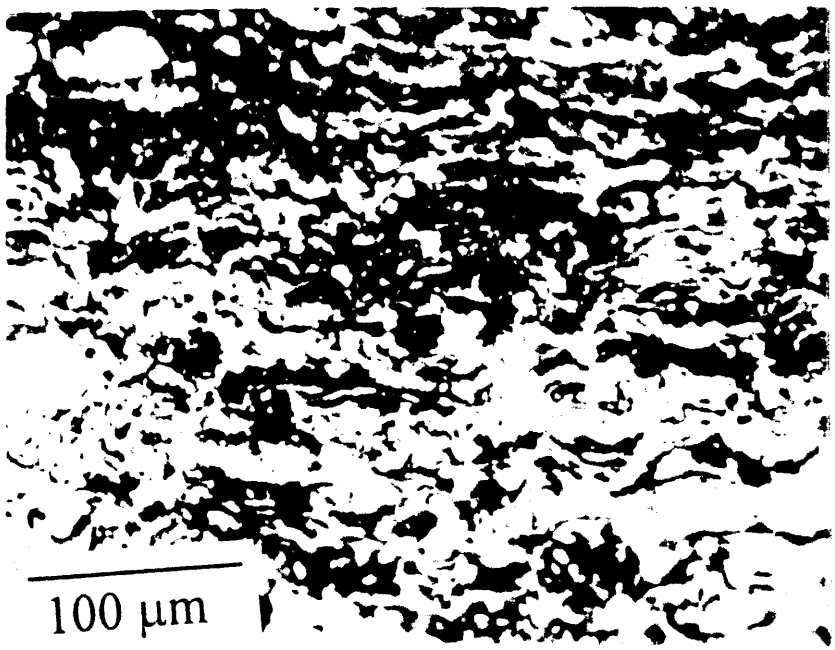

Figure 3-2: Microstructure of Ni–Al_2O_3 graded coating, showing the wavy nature of the layered deposits formed by plasma spraying. Ni is the light area, while Al_2O_3 is the darker area.

Figure 3-3: Microstructure of Ni–Al_2O_3 graded coatings showing details of the solidified Ni (lighter regions) and Al_2O_3 (darker regions) particles formed by plasma spray.

Chapter 4

Results and Discussion

In this section, we present experimental results of the evolution of internal stress and thermal mismatch stresses in homogeneous and graded layers of Ni–Al_2O_3 composites. For this purpose, we adopt two approaches.

1. First, the stresses in the coatings were determined using a thin-film approximation. The main advantage of this method is that the average stress in the coating can be determined accurately without the need for any measurement of the mechanical properties of the coating, provided that the thickness of the coating is significantly smaller that of the substrate (this approximation is not valid for some cases considered in Table 3.1.) For this purpose, the classical Stoney formula [42] for thin films is employed, as described in Section 4.1.

2. The stresses in the coatings were next determined after assessing the elastic and thermal expansion properties of the coatings. The average Young's modulus value of a coated specimen was measured using the four-point bend method outlined in Section 3.4, and the resulting values were compared with other independent measures. On the basis of this experiment, the modulus of the Ni–Al_2O_3 coating for the different cases was estimated by a simple rule-of-mixture approximation which, as described below in Section 4.3, reflects the trends in

	E (GPa)	α ($^{\circ}C^{-1}$)
Ni/5% Al	207	12×10^{-6}
Al_2O_3	380	5.4×10^{-6}
Steel	207	12×10^{-6}

Table 4.1: Properties of the constituent phases of the graded coatings and substrate.

plasma-sprayed porous coatings. Since the focus here is principally on elastic stresses, such an approximation is believed to provide an accurate description of the actual deformation response. The elastic properties so chosen for the coatings were then used to predict the internal stresses arising from deposition. It is shown that in the thin-film limit, both the Stoney approximation and the more rigorous layered material model lead to similar values of internal stresses, as anticipated, but in cases where the layer thickness of the deposits are of the order of the substrate thickness, using the thin film approximation introduces significant errors, and the more appropriate model must be used.

In addition, the processing-induced stresses were isolated from the thermal mismatch stresses that arise as a result of cooling from the processing temperature. For this purpose, the coefficient of thermal expansion was calculated using the scanning laser data for the different graded coatings.

The values of isotropic Young's modulus E and coefficient of thermal expansion α at room temperature for the steel substrate and the bulk constituent phases of the coatings, i.e., Ni-5%Al and Al_2O_3, are listed in Table 4.1. In the temperature range 20°C to 150°C (i.e., the deposition temperature), these properties were assumed to be independent of temperature. The average Poisson ratio, ν, of the coating was taken to be constant through the thickness, with a value of 0.32.

4.1 Determination of Residual Stresses Using the Thin-Film Approximation

The average stress in a single layer of a thin coating deposited on a steel substrate was calculated using the curvature change of the material during processing, the bulk properties of the steel substrate, and the thickness of the substrate and the deposited layer. One such monolayer specimen consisted of a single layer of nickel deposited on the steel substrate. The remaining layers were graded in 20% increments of Al_2O_3 composition, with one layer ranging from 0 to 20% Al_2O_3 in nickel, and the others ranging from 20–40%, 40–60%, 60–80%, and 80–100% Al_2O_3 in nickel (see Table 3.1). The biaxial stiffness of the beams, I_{bi}, was calculated using the height, h_0, of the substrate, and the Young's modulus E and Poisson's ratio ν of the steel substrate.

The stiffness of the beam was then used to calculate the average stress in the deposited layer, using the thin-film approximation that the properties of the beam are dominated by the properties of the thick steel substrate, so that the neutral axis of the beam, defined as the location where the strain is equal to zero when a pure mechanical bending moment is applied to the specimen, is located at $z_N = h_0/2$. Here, $\Delta\kappa$ is the change in curvature from a substrate with no deposit to a substrate with a coating layer deposited on it, Δh is the change in thickness from a substrate to a substrate with a coating layer, and h_0 is the substrate thickness. The classical Stoney formula for thin films [42], which was suitably modified for the present case, was used to determine the average stress in a single layer, graded thin-film coating:

$$\sigma = -\frac{I_{\text{bi}}\Delta\kappa}{(h_0 - z_N)\Delta h}. \tag{4.1}$$

The estimated average value of total internal stress at 20°C in each of the single graded deposits (with only the Ni-5%Al layer (i.e. no Al_2O_3) and layers each of

which has Al_2O_3 concentration varying between 0–20%, 20–40%, 40–60%, 60-80%, and 80-100%) is plotted in Figure 4-1, as a function of the average Al_2O_3 content. The maximum tensile internal stress of approximately 158 MPa is recorded for the Ni-5%Al layer on the steel substrate with 0% Al_2O_3. For the graded single-layer coatings, Figure 4-1 shows the stresses corresponding to the average composition of the coating (e.g., for the 40–60% Al_2O_3 coating, specimen 9 in Table 3.1, the stress is plotted at an average Al_2O_3 concentration of 50% in Figure 4-1). With an increase in Al_2O_3 content, the tensile internal stress decreases. For the single coating with the highest Al_2O_3 content (i.e. for the 80–100% Al_2O_3), the average stress becomes slightly compressive ($\sim$ –11 MPa). (This same trend for the total residual stress at room temperature was also found using the plate formulation, as shown later in Figure 4-4.)

4.2 Determination of thermal expansion coefficient

The average coefficient of thermal expansion of a graded coating deposited on a steel substrate was also determined for the above specimens. For this purpose, the change in curvature with temperature of each specimen was determined by the thermal loading experiments.

In order to properly estimate the values of Young's modulus which enter into the calculations of α and residual stresses, it is essential to have proper experimental measurements of the in-plane Young's moduli. In our own experimental measurements of compliance changes during the application of a constant bending moment using the four-point bend set up, the average Young's modulus for the specimen with fully graded coating (Specimen #6 in Table 3.1) was determined to be 54 GPa. This value is significantly smaller than the bulk Young's modulus of Ni and Al_2O_3 , which are

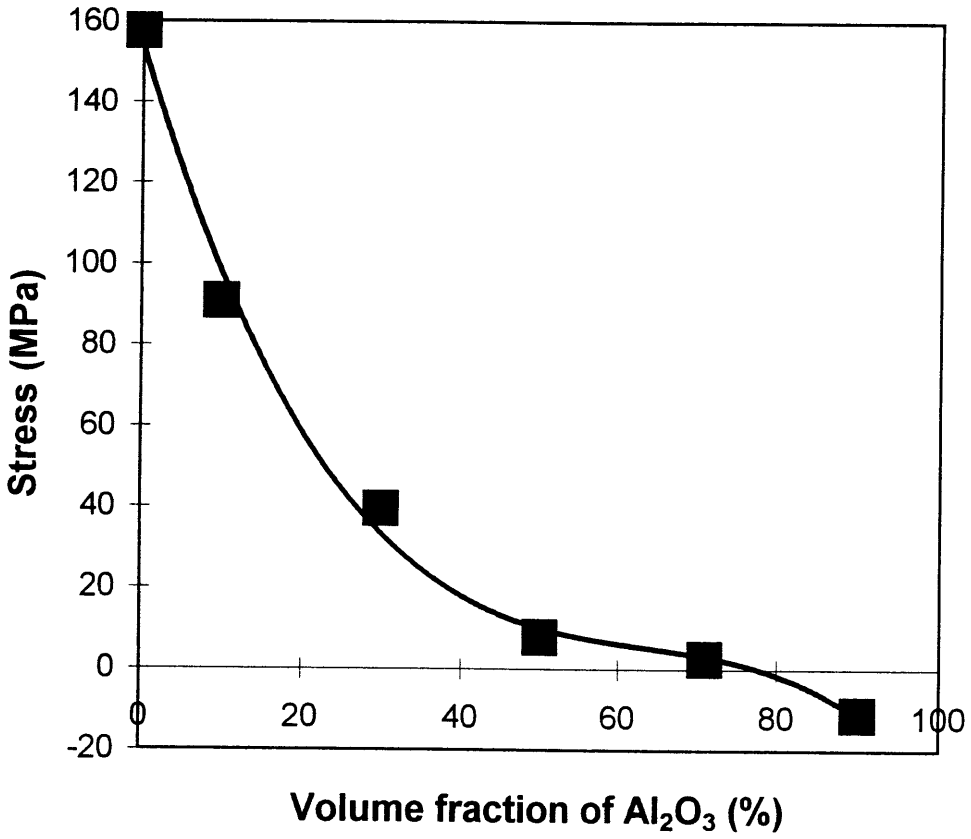

Figure 4-1: Total processing-induced residual stresses at room temperature in single graded layers of Ni–Al_2O_3, using thin film analysis.

207 GPa and 380 GPa, respectively (see Table 4.1). Thus the plasma-sprayed porous coatings used in our present study have been found to be significantly more compliant than the fully dense bulk specimens comprising the same constituent phases. This result is fully consistent with other studies (e.g., Pajares et al. [43], Hillery et al. [44], Suresh et al. [45], McPherson [46], and Sturlese et al. [47]). On the basis of this information, we have consistently chosen the values of Young's modulus for the constituent Ni and Al_2O_3 phases to be one-fifth of their respective bulk material values, for subsequent analysis. While there are likely to be small differences in the levels of porosity between the Ni-rich and alumina-rich end of the graded layer, the extent of porosity at either end was independently estimated to be in the range 8-12%.

For the purpose of estimating the CTE values of the composite coatings of Ni and Al_2O_3 shown in Table 3.1, Young's modulus was then estimated by using the rule of mixtures, with the average value of Young's modulus for each layer being proportional to the values of Young's modulus of plasma-sprayed Ni and Al_2O_3 (i.e., one-fifth of the bulk modulus value), in proportion to their composition by volume in each specimen. The experimental curvature versus temperature data from the thermal loading experiments were used to calculate the CTE, along with the rule-of-mixtures estimates of E, modified to account for the porosity of plasma-sprayed deposits.

The results of these calculations are presented in Figure 4-2, in which average coefficient of thermal expansion of each added layer is plotted versus average volume % Al_2O_3 in each layer. The values of CTE decrease with increasing Al_2O_3 composition, with a slight increase in value at the Al_2O_3–rich end. This behavior can be best understood by examining the CTE behavior of a continuous-fiber composite in the directions parallel and perpendicular to the fiber directions, as shown in the bottom and top curves, respectively, in Figure 4-3. It can be seen from the behavior of the CTE in composite materials that the behavior exhibited by the graded coatings in

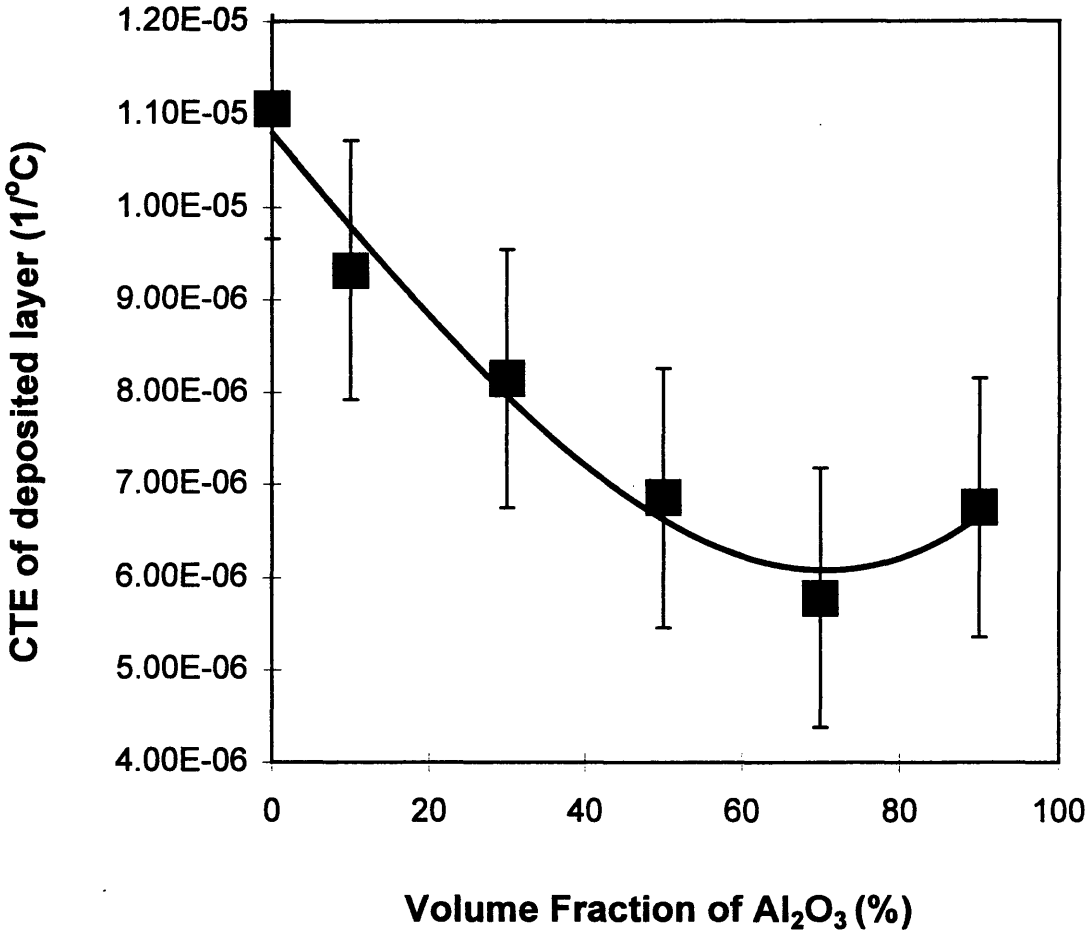

Figure 4-2: Coefficient of thermal expansion of Ni–Al_2O_3 layers as a function of layer composition.

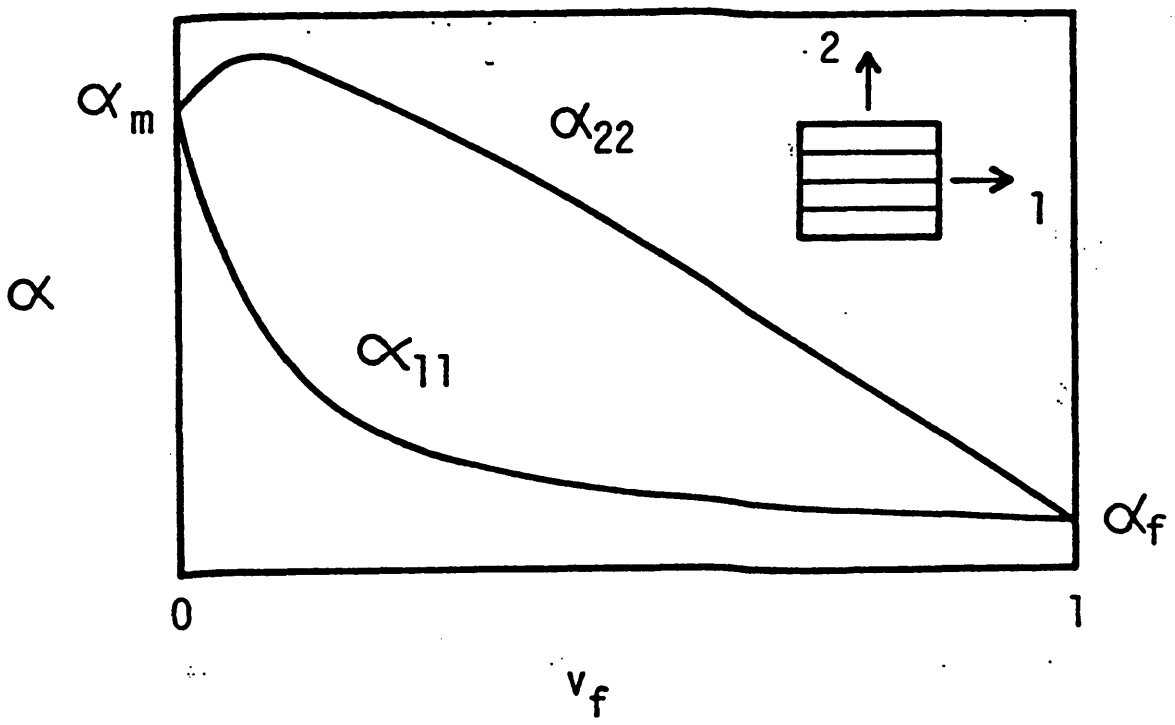

Figure 4-3: Coefficient of thermal expansion behavior of continuous fiber-reinforced composites [48].

this experiment lies intermediate between the two behaviors displayed in Figure 4-3, with our coatings exhibiting more characteristics of the CTE dependence along the fiber direction than perpendicular to it. This is to be expected, given that the deposited microstructures, while consisting of wavy and irregular splats, still were predominantly oriented in one plane–the plane parallel to the substrate (see Figures 3-2 and 3-3, for example). Thus the α behavior of our graded coatings exhibits behavior between that of the two orientations of continuous fiber composites, demonstrating that the plasma spray-deposited specimens lie somewhere between the two extremes of composite behavior given in Figure 4-3.

4.3 Determination of residual stresses using the properties of the coatings

The residual stresses at room temperature in single graded layer deposits are shown in Figure 4-4. In addition, the calculated CTE values were used along with the estimates of Young's modulus to determine the thermal mismatch stresses created upon cooling the graded materials from the processing temperature of 150°C to room temperature. From the difference between total residual stress at room temperature and the thermal mismatch stresses, the intrinsic quenching stresses due to rapid solidification at the processing temperature were also determined. The total room temperature residual stresses, intrinsic quenching stresses at the processing temperature, and thermal mismatch stress for a temperature increase of 130°C are all shown in Figure 4-4. These values for the residual stresses differ by about 30-35% from the values given in Figure 4-1, where the stress was determined by assuming a thin film deposit and calculating the resulting stress based on the modified Stoney formula. This is a good indication that the thin-film approximation is not strictly valid for the thick-layered deposits studied here, thus making the analytical method necessary for an accurate stress determination. It is also worth mentioning that the stresses in the Ni layer were measured to be near 200 MPa, a value that is within the upper end of the published range of Ni yield stress. The values for Ni yield stress in the literature range from 140-200 MPa. In the material used in our studies, the yield stress seems to be near 200 MPa, the maximum stress reached in the Ni layers. Since the analytical method presented here depends on linear elastic beam and plate theories, it does not accurately capture the behavior in places where local yielding has occurred. When plasticity occurs, in fact, the stress is likely to remain near this yielding stress rather than increasing in an elastic manner, such that the calculated solutions will probably overpredict the stresses in the yielded area of the pure metal and metal-rich graded

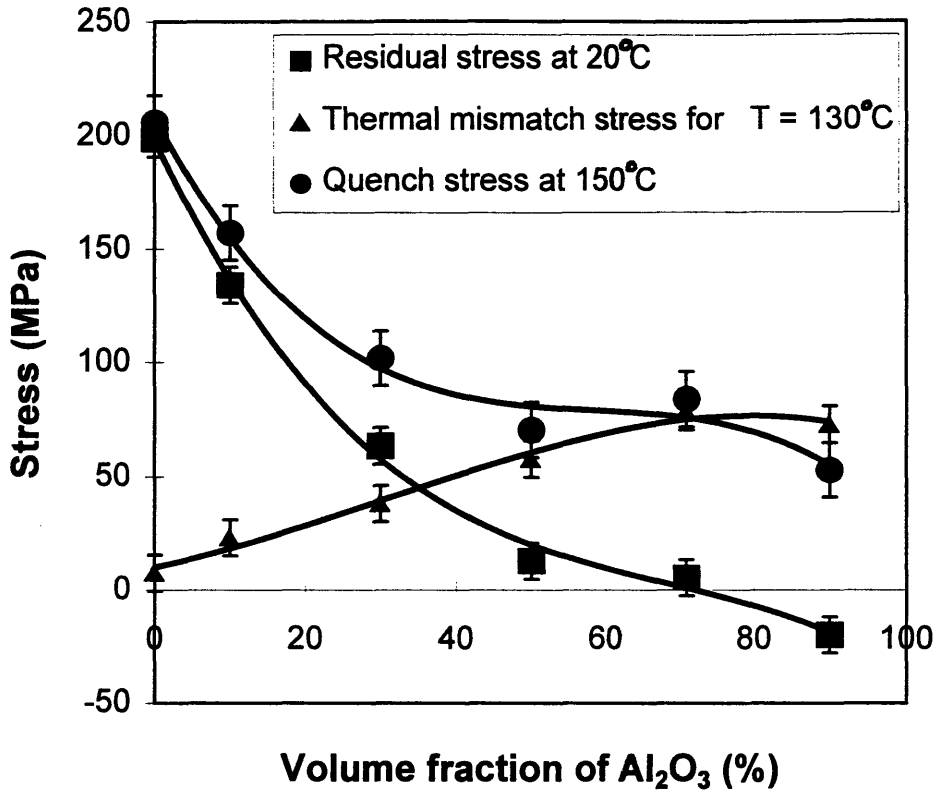

Figure 4-4: The separation of thermal mismatch, quenching, and total processing stresses in graded monolayers of Ni–Al_2O_3, using the rule of mixtures to estimate E.

area, which remain lower than their elastically predicted values.

No direct comparison with prior work is possible for the graded coatings because the present work constitutes the first experimental estimation of intrinsic stresses in metal-ceramic coatings with gradients in composition. For homogeneous coatings, the results shown in Figures 4-1 and 4-4 exhibit trends similar to other studies of residual stresses in plasma-sprayed deposits. Kuroda [18], for example, found tensile quenching stresses of approximately 140 MPa for Ni-20Cr on steel and lower stresses of about 30 MPa for plasma-sprayed Al_2O_3 on steel at deposition temperatures ranging from 60-100°C, while Kuroda and Clyne [30] found similar trends of positive quenching stresses on the order of 300 MPa for Ni and lower but still positive quenching stresses of 80–~100 MPa for Al_2O_3, at elevated processing temperatures of 400–1000°C. Howard

and Clyne [21] studied deposition of a boron carbide ceramic on a Ti alloy substrate, and found compressive residual stresses in the ceramic deposit, ranging from about –130 MPa to 0 MPa.

Chapter 5

Conclusions and Future Work

An experimental method developed as part of the author's doctoral thesis work has been used to determine the residual stresses at room temperature, the intrinsic stresses at the processing temperature resulting from the deposition process, and the coefficient of thermal expansion, as a function of depth in the deposit, for functionally graded Ni-Al_2O_3 layers deposited on a steel substrate by plasma spray deposition. It is found when Ni–Al_2O_3 composite coatings, typically 180-420 μm thickness, are plasma-sprayed onto a thick steel substrate, residual stresses as large as 200 MPa are found in the coating at room temperature. The values of in-plane Young's modulus of the graded coatings have been measured to be as low as 54 GPa. Such low E values are found to be consistent with other independent estimates of the elastic properties of plasma-sprayed materials. The CTE values of the Ni–Al_2O_3 composite coatings deposited by thermal spray are also assessed using the curvature measurement technique, and are found to be comparable to the values of the bulk properties.

The work suggests a number of future studies that would provide additional useful information in the study of layered and graded coatings. One such study suggested by this work would be a thorough and systematic experimental determination of the Young's modulus of deposited layers for each layer of a graded deposit or single-layered deposit. Such a study could be done, for example, by performing four-point

bending tests on each specimen of a series of partially-deposited graded material layers to determine the through-thickness mechanical property profile of the graded deposit. The determination of residual stresses and thermo-mechanical properties in other material systems, such as the ZrO_2 – NiCrAlY system which is widely used industrially in engine coatings, would be another valuable step towards gaining a better understanding of the behavior of layered and functionally graded materials. In addition, a similar technique could be used to determine the residual processing-induced stresses resulting from other deposition techniques, such as physical vapor deposition or electron beam deposition.

Bibliography

1. B .H. Rabin and I. Shiota, Editors, Special Issue on Functionally Gradient Materials, *MRS Bulletin* 20, 1995.

2. A. Mortensen and S. Suresh, *Inter. Mater. Rev,* 40:239, 1995.

3. A. E. Giannakopoulos, S. Suresh, M. Finot, and M. Olsson, *Acta Metall. Mater.,* 43:1335, 1995.

4. M. Finot, S. Suresh, C. Bull, and S. Sampath, *Mat. Sci. Eng. A,* 59, 1996.

5. E. Weissenbek, H. E. Pettermann, and S. Suresh, *Acta Mater., in press*, 1996.

6. R. L. Williamson, J. K. Wright, and K. J. Maggs, *Mat. Sci. Eng.*, 187:87, 1994.

7. J. T. Drake, R. L. Williamson, and B. H. Rabin, *J. Appl. Phys.* 74:1321, 1993.

8. E. A. Fitzgerald, Y.-H. Xie, D. Monroe, P. J. Silverman, J.-M. Kuo, A. R. Kortar, F. A. Thiel, B. E. Weir and L. C. Feldman, *J. Vac. Sci. and Technol.*, B10:1807, 1992.

9. Soc. for Experimental Mechanics, *Handbook of Measurement of Residual Stresses*, Ed. Jian Lu, Fairmount Press, Inc., Lilburn, GA, 1996.

10. T. W. Clyne and S. C. Gill, *J. Therm. Spray Technol.*, 5(4):401, 1996.

11. M. Gudge, D. S. Rickerby, R. Kingswell, and K. T. Scott, *Proc. 3rd Int'l Therm. Spray Conf.*, pp. 331-337, Long Beach, CA, 1990.

12. D. J. Greving, E. F. Rybicki, and J. R. Shadley, *Proc. 7th Nat'l. Spray Conf.*, pp. 647-653, Boston, MA, 1994.

13. P. Bialucki, W. Kaczmar, and J. Gladysz, *Advances in Thermal Spraying; Proc. 11th Int'l Therm. Spray Conf.*, p. 837, Welding Institute of Canada, Pergamon press, 1986.

14. M. K. Hobbs and H. Reiter, *Thermal Spray: Advances in Coatings Technology*, pp. 285-290, ASM, 1988.

15. S. C. Gill and T. W. Clyne, *Metall. Trans. B*, 21:377, 1991.

16. S. C. Gill and T. W. Clyne, *Proc. 7th Nat'l Spray Conf.*, pp. 581-586, Boston, MA, 1994.

17. S. C. Gill and T. W. Clyne, *Thin Solid Films*, 250:172, 1994.

18. S. Kuroda, Colloquium, SUNY, Stonybrook, NY, 1996.

19. A. L. Shull, H. G. Zolla, and F. Spaepen, *Proc. MRS Fall'94 Symp. on Thin Films: Stresses and Mechanical Properties V*, Boston, MA 1994.

20. T. W. Clyne and Y.C. Tsui, *3rd Int'l. Symp. on Structural and Functional Gradient Materials*, Lausanne, Switzerland, 1994.

21. S. J. Howard and T. W. Clyne, *Proc. 7th Nat'l Spray Conf.*, Boston, MA, 1994.

22. A. C. Leger, A. Grimaud, P. Fauchais, and C. Catteau, *National Thermal Spray Conf., in press*, 1996.

23. N. Tani, T. Ishida, M. Kawano, and K. Kamachi, *Advances in thermal spraying: Proc. 11th Int'l Therm. Spray. Conf.*, p.605, Welding Institute of Canada, Pergamon Press, 1986.

24. S. Tobe, H. Misawa, K. Akita, and Y. Kon, *Proc. 7th Nat'l Therm. Spray Conf.*, Boston, MA, 1994.

25. H. Zhuong and T. Zhang, *2nd Plasma Technik Symp.*, 3:331.

26. R. Knight and R. W. Smith, *Proc. 6th Nat'l Spray Conf.*, pp. 607-612, Anaheim, CA, 1993.

27. Q. Ma and D. R. Clarke, *Acta Metall. Mater.*, 41:1811, 1993.

28. Q. Ma and D. R. Clarke, *Acta Metall. Mater.*, 41:1817, 1993.

29. L. B. Freund, *J. Mech, Phys. Solids*, 44:723, 1996.

30. S. Kuroda and T. W. Clyne, *Thin Solid Films*, 200:49, 1991.

31. M. Finot and S. Suresh, *J. Mech. Phys. Solids*, 44:683, 1996.

32. S. Ho and E. J. Lavernia, *Metall. and Mater. Trans. A*, 27A:3241, 1996.

33. S. Parthasarathi, B. R. Tittmann, K. Sampath, and E. J. Onesto, *J. Therm. Spray Technol.*, 4:367, 1995.

34. E. F. Rybicki, J. R. Shadley, Y. Xiong, and D. J. Greving, *J. Therm. Spray Technol.*, 4:377, 1995.

35. S. H. Leigh, C. K. Lin, S. Sampath, H. Herman, and C. C. Berndt, *Proc. Int'l Therm. Spray Conf.*, pp. 945-950, Kobe, 1995.

36. C.-C. Chiu and E. D. Case, *Mat. Sci. and Eng.*, A132:39, 1991.

37. C.-C. Chiu, *Mat. Sci. and Eng.*, A150:139, 1992.

38. T. P. Weihs, S. Hong, J. C. Bravman, and W. D. Nix, *Mat. Res. Soc. Symp. Proc.*, 130:87, 1989.

39. M. Finot, O. Kesler, and S. Suresh, *Method and apparatus for the evaluation of a depth profile of thermo-mechanical properties of material and coatings*, MIT case no. 7358, Cambridge, MA, U.S. Patent filed July 1996.

40. O. Kesler, M. Finot, S. Suresh, and S. Sampath, *Acta Mater., in press*, 1997.

41. O. Kesler, MIT Doctoral Thesis, work in progress, 1997.

42. G. G. Stoney, *Proc. R. Soc. London Ser. A*, 82:172, 1909.

43. A. Pajares, L. Wei, B. Lawn, N. Padture, and C. Berndt, *Mater. Sci. Eng.*, A208:158, 1996.

44. R. V. Hillery, B. H. Pilsner, R. L. McKnight, T. S. Cook, and M. S. Hartle, NASA Contractor Report 180807, 1988.

45. S. Suresh, A. E. Giannakopoulos, and J. Alcala, *Acta Mater., in press*, 1996.

46. R. McPherson, *Proc. 5th Conf. Aluminum Oxide* (Prague, Czechoslovakia: Prague Inst. of Chem. Tech.), 1, 1990.

47. S. Sturlese, R. Dal Maschio, G. Bartuli, N. Zacchetti, and M. Berardo, *High Performance Ceramic Films and Coatings*, ed. P. Vicenzini, Elsevier Science Publish., 353, 1991.

48. P. K. Mallick, *Fiber-Reinforced Composites*, 2nd Ed., Marcel Dekker, NY, 1993.